AIAA 80-1803R

# Vortex-Lattice Method for the Calculation of the Nonsteady Separated Flow over Delta Wings

Daniel Levin* and Joseph Katz†
*NASA Ames Research Center, Moffett Field, Calif.*

**An analysis is made of the wake structure and the forces on a delta wing as it undergoes nonsteady motion, wherein the flow separates at the leading edge. Comparisons of these predictions with existing experimental and theoretical data for the nonsteady linear and nonlinear motions indicate good agreement. It was found that the time-dependent, wake-shedding numerical procedure applied here for the wake rollup and the lift force calculation resulted in considerable saving of computer time over methods using the iterative wake rollup procedure. Calculated results for various motions of the delta wing, including the plunging motion, are presented for both the separated and the attached flow cases.**

## Nomenclature

$A_{ij}$ = influence coefficient
$a_p$ = panel chord
$AR$ = aspect ratio
$B_{ij}$ = influence coefficient
$b(x)$ = local wing span
$C_{ij}$ = influence coefficient
$C_L$ = lift coefficient
$C_p$ = $(P-P_\infty)/\frac{1}{2}\rho U^2$ pressure coefficient
$c$ = wing chord
$F$ = normal force
$h$ = panel vertical distance from $x$ axis
$P$ = pressure
$p$ = angular velocity about $x$ axis
$q$ = angular velocity about $y$ axis
$r$ = angular velocity about $z$ axis
$S$ = wing area
$t$ = time
$U$ = wing forward velocity
$u$ = induced velocity to the $x$ direction
$v$ = induced velocity to the $y$ direction
$w$ = induced velocity to the $z$ direction
$x,y,z$ = wing coordinates
$\alpha$ = angle of attack
$\Gamma$ = circulation
$\Gamma_f$ = wing bound circulation
$\Gamma_s$ = separated wake circulation
$\Gamma_w$ = trailing edge wake circulation
$\rho$ = density
$\phi$ = velocity potential

*Subscripts*

0 = at $t=0$
$\infty$ = steady-state value
$w$ = wake

## Introduction

THE lifting characteristics and wake structure of highly swept back and delta wings with sharp leading edges have lately attracted increased interest. This is partially due to the desirable performance characteristics of those wings both at high supersonic cruise and at low subsonic short takeoff and landing conditions. The low-speed, high-lift condition is obtained with the aid of two strong vortices which emanate from the sharp leading edges of the wing. During certain low-speed maneuvers these leading-edge vortices might move and interact with the aircraft control surfaces, causing nonlinear stability derivatives. Analytical studies based on nonsteady aerodynamics of these conditions are still very limited, but this approach can significantly increase the understanding of some critical flight conditions (e.g., departure or stall spins).

Lifting surface methods based on steady aerodynamics for the calculation of leading-edge separated flows are now fairly well developed and are capable of solving the flow about complex geometries such as wing canard combinations.[1,2] An extensive list of the literature covering this subject is summarized in three recent reviews. The first (Johnson and Tinoco[3]) is based on the experience of the Boeing Company that developed its own code. The second (Lamar and Luckring[4]) provides both experimental and theoretical data on configurations utilizing vortex flows. The third[5] is a description and an analysis of the inviscid flow models that are being used to represent three-dimensional separation of vortex type. The major disadvantage of those codes is the large amount of computer time required for complex wake geometries, since the final bound vorticity and wake rollup is obtained by an iterative technique. Moreover, the first assumed vortex wake shape which starts the iterative procedure should be close to the final solution to eliminate a possible convergence to an undesirable solution. The mathematical existence of such multiple solutions for the wake position in the two-dimensional crossflow was shown by Weihs and Boasson[6] in their study of the location of separated vortex wakes behind slender bodies. Most of the current iterative methods report that the first guess for the vortex wake does not effect the final solution, but may increase substantially the computation time.

A time-dependent wing-following, wake-shedding procedure can provide both transient and asymptotic wake shapes and wing loadings without utilizing the iterative method. A similar method was developed by Djojodihardjo and Widnall[7] and was used later by Summa to solve complex wake shapes behind impulsively started helicopter rotors[8] and wings.[9] These codes allow vortex rollup from side edges and wing tips but not leading-edge separation.

A study of the unsteady aerodynamic loads with allowance for leading-edge separation was reported by Atta et al.,[10] Kandil et al.,[11] and Kandil.[12] They performed calculations for several nonsteady motions such as constant rolling[11] and pitching oscillation[10] and developed a special triangular leading-edge panel to allow leading-edge separation. An important feature of their model is the calculation of the pressure distribution about the wing with the local velocity distribution; that is, both forces and downwash for the boundary condition were calculated at the collocation points

Presented as Paper 80-1803 at the AIAA Aircraft Systems Meeting, Anaheim, Calif., Aug. 4-6, 1980; submitted Sept. 10, 1980; revision received April 21, 1981. This paper is declared a work of the U.S. Government and therefore is in the public domain.

*NRC Associate. Member AIAA.
†NRC Associate.

while other methods utilize the quarter panel vortex location for force calculation and the three-quarter panel collocation point for the boundary condition. However, the nonsteady vortex rollup was calculated by a complex iterative method,[10] and the inclusion of the velocity potential derivatives in the Bernoulli equation is not reported clearly.

The sudden acceleration of delta and rectangular wings was studied by Rehbach[13] and Belotserkovskiy and Nisht,[14] who calculated oscillatory leading-edge separation for the two-dimensional case. However, Rehbach's calculations show some numerical oscillations, while the practical information on the calculational code used in Ref. 14 is minimal.

In the present study, a vortex-lattice code was developed for calculating the steady and unsteady flow about a three-dimensional thin wing, with or without leading-edge separation. Both leading-edge and trailing-edge wake rollup are determined numerically by a time-dependent vortex-shedding procedure that does not require an iterative technique as do most present steady-state solutions. This considerably reduces the computational effort since the final number of wake elements is obtained only at the latest time step. Furthermore, the present method can provide transient aerodynamic loads and wake geometries during the time-dependent motion and improves the understanding of some vortex interaction problems.

## Method

Vortex-lattice methods as well as the present method assume that viscous effects can be accounted for by proper modeling of the flow. That implies that information such as the location of separation lines and the strength of the shed vorticity is to be supplied by an experiment, flow visualization, or viscous flow calculations. When such information is provided to the potential flow model, the wake rollup and pressure distribution about the wing can be calculated. The basic assumption of such a model is that the flow is incompressible, irrotational, and homogeneous over the whole fluid region excluding the wing and its wake. Therefore a velocity potential exists and the continuity equation becomes

$$\nabla^2\phi = 0 \tag{1}$$

with the following boundary conditions stated in an inertial frame of reference. 1) There is no flow across the wing surface. 2) The induced velocity of the wing decays far from the wing, everywhere except near the wakes. The extension of the method into the time-dependent framework requires the application of Kelvins theorem where zero net circulation is specified for all time intervals:

$$\frac{d\Gamma}{dt} = 0 \tag{2}$$

### Vortex-Lattice Model

A possible solution for the lifting problem stated above is derived in Refs. 15 and 16, and a schematic description of the model based on those principles is shown in Fig. 1. The basic lifting panel consists of a bound vortex, which is a partial solution of Eq. (1) located at the quarter-chord, and the collocation point is at the three-quarter chord of the centerline. The triangular leading-edge section was investigated in Ref. 2 and was found to satisfactorily simulate leading-edge separation. In addition, the separated vortex strength $\Gamma_{s_i}$ is adjustable to simulate various leading-edge radii. In the present study, however, sharp leading edges were assumed; consequently, the leading-edge separated vortex strength was set equal to the corresponding triangular panel strength $\Gamma_{f_i}$.

The vortex-lattice model in Fig. 1 is already fulfilling boundary condition (2) for Eq. (1) since its induced velocity decays with increased distance. Equation (2) is fulfilled at any time by constructing the bound and wake circulation elements from closed vortex rings as shown in Fig. 1. Boundary condition (1) for Eq. (1) is satisfied while deriving the integral equation[16] to calculate the strength of the bound circulation $\Gamma_{f_i}$ associated with each panel:

$$-[U-ry_i]\sin\alpha_i - qx_i + py_i + \frac{\partial h_i}{\partial t} = [A_{ij}]\begin{bmatrix}\Gamma_{f_1}\\ \vdots\\ \Gamma_{f_i}\\ \vdots\\ \Gamma_{f_n}\end{bmatrix} + [B_{ij}]\begin{bmatrix}\Gamma_{w_1}\\ \vdots\\ \Gamma_{w_i}\\ \vdots\\ \Gamma_{w_m}\end{bmatrix} + [C_{ij}]\begin{bmatrix}\Gamma_{s_1}\\ \vdots\\ \Gamma_{s_i}\\ \vdots\\ \Gamma_{s_l}\end{bmatrix} \tag{3}$$

Here $(p,q,r)$ is the rotational motion around the $(x,y,z)$ axes correspondingly, $U(t)$ is the momentary far-field velocity, and $\alpha_i$ is the panel angle of attack. The heaving motion of the panel relative to the $(x,y,z)$ axes is $h_i(t)$, and its effect on the downwash is the $\partial h_i/\partial t$ term in Eq. (3). The first term on the right, $A_{ij}$, stands for all the influence coefficients resulting from the Biot Savart bound vortex influence calculations.[17] The second and third terms $B_{ij}$ and $C_{ij}$ represent the influence coefficients of the trailing-edge wake $\Gamma_{w_i}$ and loading-edge separated elements $\Gamma_{s_i}$, and their strength is known from previous time steps. Equation (3) is derived for all $n$ panels on their collocation points resulting in $n$ equations with $n$ unknown $\Gamma_{f_i}$ at each time interval. If wing shape is not varying during flight (flap motion ailerons, etc.) the coefficients $A_{ij}$ are constant and their calculation is performed only once. The calculational effort of $B_{ij}$ and $C_{ij}$ increases with time as the number of wake elements grows. This must be performed at each time interval since wake rollup changes the geometry involved in its induced velocity calculations.

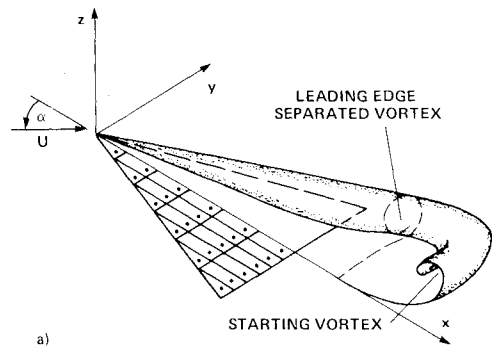


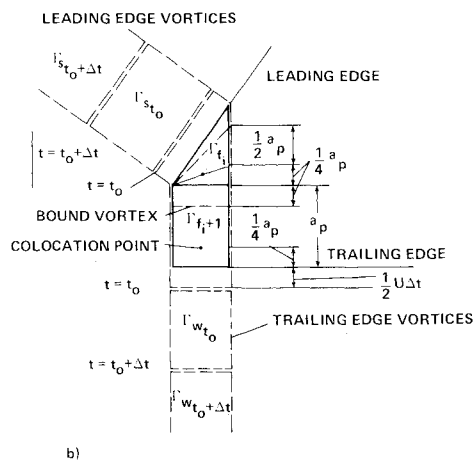


**Fig. 1 Schematic of vortex-lattice method and panel geometry.**

**Calculational Procedure**

To demonstrate the calculational procedure it is assumed that at $t=0$ the wing was set suddenly into motion. The first calculation takes place at $t=t_0$ as it is shown in Fig. 1b, and the spanwise wake vortex is placed in the midinterval traveled ($\frac{1}{2}\ U\Delta t$). For the linear (not separated) transient calculation there is no direct coupling between the panel length $a_p$ and the time step, but for more precise accuracy the nondimensional time step should be smaller than 0.2 ($\Delta tU/c<0.2$). For separated flow, however, it is recommended that the time steps and the panel lengths should be of the same order of magnitude ($\Delta tU/a_p \simeq 1$) to prevent the separated wake elements from being too close to the wing collocation points.

After the first time step the momentary position and angular motion of the wing are known and the geometrical boundary condition for the downwash [left side of Eq. (3)] is determined. Then the influence coefficients $A_{ij}$ are calculated while $B_{ij}=C_{ij}=0$ for the first time step, since there are no free wake elements shed as yet. At this point the bound vorticity strength $\Gamma_{f_i}$ is solved and the wake rollup step is performed by moving the wake points shed at $t=t_0$. The downwash at each vortex edge location $(u,v,w)_i$ is calculated by Eq. (4), which is similar to the right-hand side of Eq. (3), but here $A_{w_{ij}}$, $B_{w_{ij}}$, and $C_{w_{ij}}$ are the influence coefficients relative to those vortex edges:

$$(u,v,w)_i = [A_{w_{ij}}]\begin{bmatrix}\Gamma_{f_1}\\ \vdots\\ \Gamma_{f_i}\\ \vdots\\ \Gamma_{f_n}\end{bmatrix} + [B_{w_{ij}}]\begin{bmatrix}\Gamma_{w_1}\\ \vdots\\ \Gamma_{w_i}\\ \vdots\\ \Gamma_{w_m}\end{bmatrix} + [C_{w_{ij}}]\begin{bmatrix}\Gamma_{s_1}\\ \vdots\\ \Gamma_{s_i}\\ \vdots\\ \Gamma_{s_l}\end{bmatrix} \tag{4}$$

Here the number of separated wake, trailing-edge wake, and wing vortex elements is $l$, $m$, and $n$, respectively. The motion of the vortex tip point $(\Delta x,\Delta y,\Delta z)_i$ is then calculated by the use of Eq. (5):

$$(\Delta x,\Delta y,\Delta z)_i = (u,v,w)_i \Delta t \tag{5}$$

To conclude the calculational procedure for a given time step, the forces acting on the foil are determined by applying the nonsteady Bernoulli's equation as derived in Ref. 16. That is,

$$\frac{P_\infty - P}{\rho} = (U-ry)\frac{\partial\phi}{\partial x} + \frac{\partial\phi}{\partial t} + \frac{1}{2}\left[\left(\frac{\partial\phi}{\partial x}\right)^2 + \left(\frac{\partial\phi}{\partial y}\right)^2 + \left(\frac{\partial\phi}{\partial z}\right)^2\right] \tag{6}$$

By integrating the pressure along a given panel with length of $\Delta x_i = x_{i+1} - x_i$ and by neglecting smaller terms $[U(t) \gg (\partial\phi/\partial x), (\partial\phi/\partial y), (\partial\phi/\partial z)]$ and assuming $r=0$ for the present calculation, the following expression for the normal force per unit width on the panel can be derived:

$$\Delta F_i = 2\rho\left(U\int_{x_i}^{x_{i+1}} \frac{\partial\phi}{\partial x}\,dx + \int_{x_i}^{x_{i+1}} \frac{\partial}{\partial t}\int_0^x \frac{\partial\phi}{\partial x}\,dx\,dx\right)$$

$$\simeq \rho\left\{U\Gamma_{f_i} + \frac{\partial}{\partial t}\left[\left(\sum_{k=1}^{i}\Gamma_{f_k} + \sum_{k=1}^{i+1}\Gamma_{f_k}\right)\frac{\Delta x}{2}\right]\right\} \tag{7}$$

Here the summation

$$\sum_{k=1}^{i}\Gamma_{f_k}$$

is performed along the chordline only, starting at the leading-edge panel ahead of the panel that its normal force $\Delta F_i$ is to be calculated. The momentary lift and drag coefficient (assuming no leading-edge suction for the separated flow) is then derived as

$$C_L = \sum_{i=1}^{n}\Delta F_i\cos\alpha_i \Big/ \frac{1}{2}\rho U^2 S \tag{8}$$

$$C_D = \sum_{i=1}^{n}\Delta F_i\sin\alpha_i \Big/ \frac{1}{2}\rho U^2 S \tag{9}$$

where $S$ is the wing area.

Once the above described calculation is completed, a time increment $\Delta t$ is added and the wing is advanced to its new location. Then a vortex ring is shed both at the trailing- and leading-edge panels, as shown in Fig. 1. The strength of the latest shed vortex ring is set equal to the shedding vortex strength at the previous time step. The schematic shedding procedure shown in Fig. 1 is actually performed over the whole wing and the number of panels used was considerably more (15-55) than indicated in the drawing. As the wake shedding process is completed, the bound vorticity is calculated by Eq. (3), the wake rollup performed with Eq. (5) and the forces acting are indicated by Eqs. (8) and (9). The above calculational scheme is then repeated for the additional time intervals. This scheme is numerically stable since iterative calculations are not required and, even with a reasonably high number of wing panels and wake elements, the vortex core distance from collocation points is far from being critical. Safeguards against singularity of Biot-Savart law are also being used.

## Results

The nonsteady separated flow over delta wings has not been widely explored; thus both analytical and experimental data are very limited. Therefore, prior to presenting the calculated results of this flow, comparison is made with simpler flow situations. The first case is the calculation of the attached

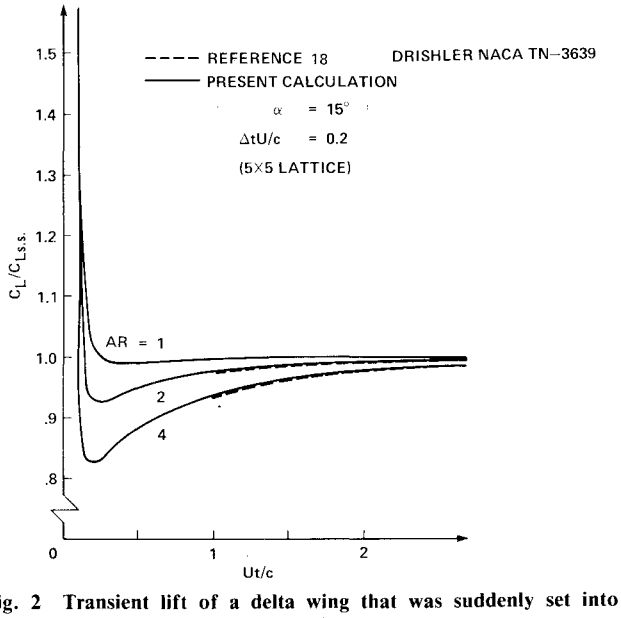


**Fig. 2 Transient lift of a delta wing that was suddenly set into motion (without leading-edge separation).**

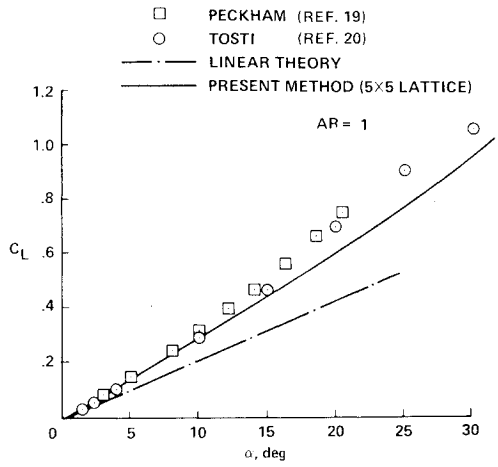


**Fig. 3 Comparison of the steady-state lift coefficient of a delta wing with leading-edge separation to published data.**

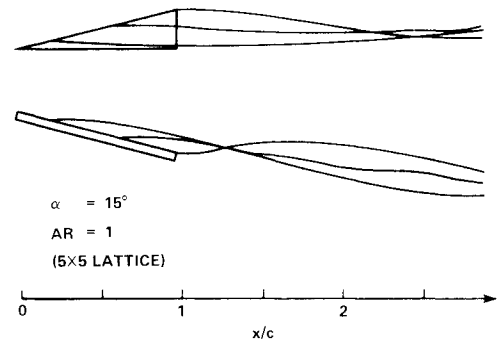


**Fig. 4 Calculated shapes of separated vortex wake cores behind a delta wing.**

flow, and the resulting lift for an impulsively started delta wing. The second case is the steady flow over a delta wing with leading-edge separation.

### Impulsively Started Wing (Not Separated Flow)

The transient loading of wings, after they have been impulsively started from rest, has been studied by Drishler.[18] His calculated results for a delta wing of various aspect ratios $\mathcal{R}$ are presented in Fig. 2 by the dashed lines. The present method not only agrees well with these data, but also provides information about the lift forces immediately after the motion was started ($Ut/c<1$). The high-lift forces at the beginning of the motion are due to the fluid acceleration, that is, the $\partial\phi/\partial t$ term in Eq. (6). As the wing obtained its final velocity the lift is reduced owing to the downwash of the shed starting vortices whose strength is decreasing as the motion continues. Consequently, the wing lift is growing until the steady-state value $C_{L_\infty}$ is obtained. The effect of the wing span or $\mathcal{R}$ is shown here as well. As the $\mathcal{R}$ is decreased, the relatively longer wing chord-to-span ratio results in a further trailing-edge vortex positioning and less downwash on the wing. Therefore the lift reduction at the beginning of the motion is larger for wings having larger aspect ratios.

### Separated Flow Over Delta Wings

In this section a comparison is made between data appearing in the literature and data calculated by the present method. The flow is assumed to be steady and the leading-edge vortices roll up and form two large vortex systems above the wing (see Fig. 1). The calculated lift coefficient values $C_L$ for a delta wing of $\mathcal{R}=1$ is shown in Fig. 3. The dashed lines represent values obtained by linear theory, where no leading-edge separation was assumed. Therefore the difference between those tow lines is the vortex lift due to the presence of

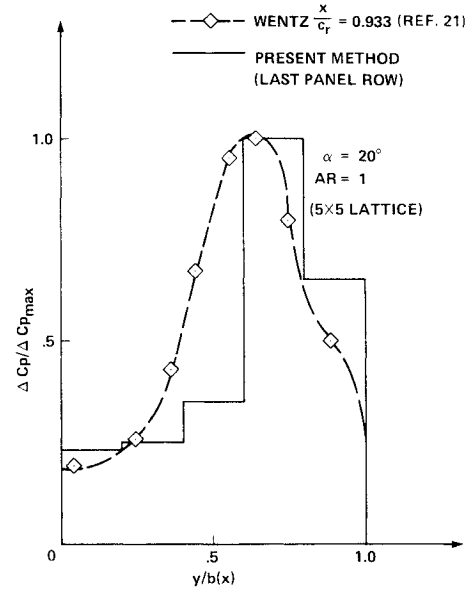


**Fig. 5 Spanwise lift distribution of a delta wing with leading-edge separation.**

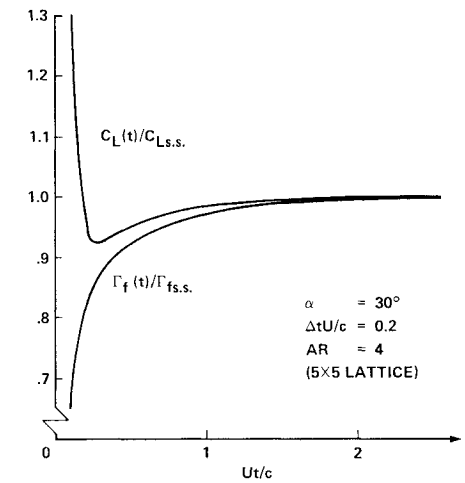


**Fig. 6 Transient lift and circulation of a delta wing with leading-edge separation.**

the two rolled-up vortex sheets above the wing. Experimental results[19,20] are also presented in Fig. 3 to show the close agreement between the present theory and experiment. The results obtained by the new method are the same as those obtained by a steady-state vortex-lattice method using an iterative process, with the same number and configuration of panels. Both results are represented by the solid line in Fig. 3. Higher agreement, to a certain degree, with experimental data could be achieved by utilizing a higher number of panels[10] and by allowing separation of inner vortices[2,5] to represent the formation of a secondary vortex sheet. For the sake of comparing the steady iterative model with the new unsteady approach, the current (5 × 5) lattice proves to be adequate.

The calculated results of the present method (shown in Fig. 3) were obtained by setting the wing suddenly into motion and proceeding with the calculational procedure until steady state is achieved. This technique has the advantage that the separated vortex core shape (Fig. 4) is determined by the wake shedding procedure as the wing is advanced into the flow. Therefore the separated vortex core position is not subject to an iterational method that might cause convergence to a nonphysical core shape. Moreover, the computational times are about one-half of the time required by the methods which use the iterative wake rollup calculation method.[2]

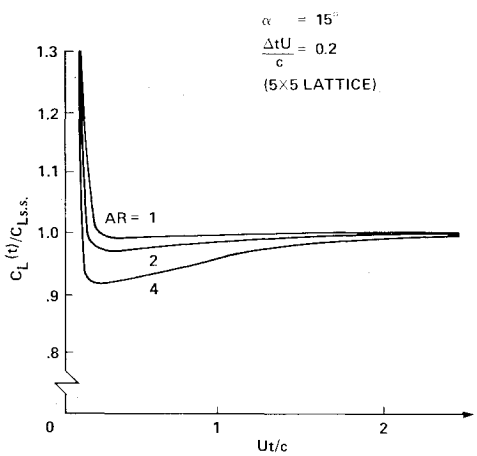


**Fig. 7 Transient lift of delta wings having various aspect ratios (with leading-edge separation).**

The spanwise load distribution of the last panel row is shown in Fig. 5. For comparison, the experimental data taken near the trailing edge by Wentz[21] was added. The normalization used here, $\Delta C_p/\Delta C_{p_{max}}$, was chosen since the panel lift represents the lift of a large section (0.2 chord length in this case), while the experimental data are relevant for a certain cross section only and because the data in Ref. 21 are for a wing with $\mathcal{R} \cong 1.146$. However, in view of the good prediction of the lift (Fig. 3) the prediction of the spanwise loading in Fig. 5 is satisfactory.

#### Nonsteady Separated Flow

The transient lift and circulation for a delta wing with leading-edge separation is shown in Fig. 6. Here the wing was accelerated from rest to its final velocity $U$ along a distance of 0.1 chord. It is assumed for the numerical calculation that the leading-edge separation is initiated at the beginning of the motion; under nonsteady conditions, however, the separation usually is delayed. The additional vortex sheets separated at the leading edge reduce the response time of the vortices shed at the trailing edge. This effect is emphasized when comparing Figs. 2 and 7, which show the lift of the separated wings is always higher. The resulting wing circulation $\Gamma_f(t)$ growth with time is shown in Fig. 6 and about 95% of the steady-state value is obtained after the wing traveled one chord length.

The effect of $\mathcal{R}$ on the nonlinear (separated flow) case is similar to the effect observed in attached flow (Fig. 2), i.e., the response time increases with $\mathcal{R}$ and the lift losses are larger. However, the results presented in Fig. 7 are offset compared to Fig. 2 owing to the additional effect of the separated vortex sheet, as explained above.

The transient forces due to various motions of a triangular surface used as an all flying canard are shown in Fig. 8. The surface having an $\mathcal{R}$ of unity and its hinge for the pitching motion is located at its apex. At the beginning of the motion the foil was accelerated along a distance of 0.1 chord to its final velocity $U$ and the angle of attack was held constant ($\alpha = 15$ deg). After a distance of 1.5 chord sinusoidal pitching motion (Fig. 8a) and a gradual change in angle of attack (Fig. 8b) were imposed. For the case of pitching motion a phase difference is noticed as a result of the downwash due to the rotational motion that affects the boundary condition on the foil in Eq. (3). The small peaks following the abrupt changes in angle of attack (i.e., at $Ut/c = 1.5$) are the forces due to acceleration and the magnitude is determined by $\Delta\alpha/\Delta t$. That is, a gradual and uniform change in $\alpha$ is assumed over the time interval $\Delta t$. Therefore, for faster variation in angle of attack, smaller time steps are required. The comparison of Figs. 8a and 8b shows the advantage of the smooth sinusoidal motion ($\partial\alpha/\partial t$ is continuous) relative to the abrupt changes in angle of attack, when vibration-free lift response is required.

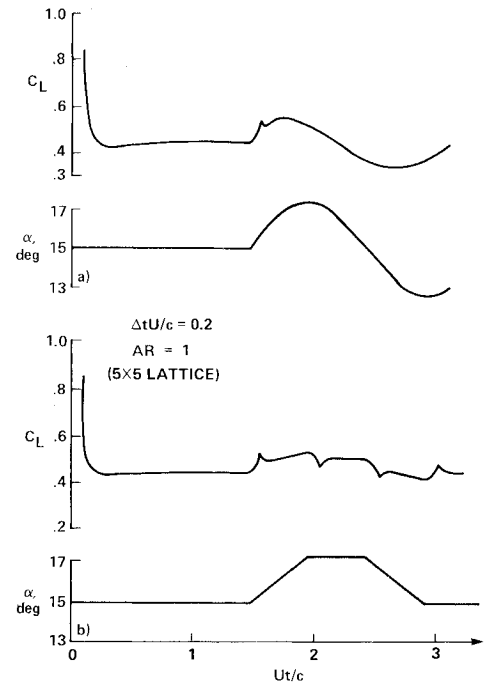


**Fig. 8 Time-dependent lift of a delta wing performing a) sinusoidal motion and b) abrupt change in angle of attack.**

## Concluding Remarks

A nonsteady vortex-lattice method was applied to solve the flow about delta wings with leading-edge separation. It was found that the lift response to abrupt changes in the wing velocity is faster for the separated flow case than for the attached flow. Similar behavior is observed when comparing the cases of leading-edge separation with those having attached flow. The minimal $C_L/C_{L_\infty}$ during the transient period is smaller for increasing $\mathcal{R}$ and the transient period is larger.

The present method was compared to a steady-state iterative method with the same panel configuration. Both codes yielded the same results for delta wings with or without leading-edge separation. Both codes were run on the same computer (CDC 7600) and were programmed with comparable efficiency. The nonsteady approach required less computer time and supplied the transient period characteristics.

Further extension of the above method with the inclusion of an aircraft dynamic equation can result in a more powerful calculational prediction. This will facilitate understanding of the time-dependent deformation of shed vortex sheets, their influence on the control surfaces, and the resulting aircraft motion. As a result, some nonlinear flight conditions, such as stall spin, could be further explored.

## References

[1] Kandil, O.A., Mook, D.T., and Nayfeh, A.H., "A Numerical Technique for Computing Subsonic Flow Past Three Dimensional Canard-Wing Configurations with Edge Separations," AIAA Paper 77-001, 1977.

[2] Rom, J., Almusnino, D., and Zorea, C., "Calculation of the Non-Linear Aerodynamic Coefficients of Wings of Various Shapes and Their Wakes, Including Canard Configurations," *Proceedings of the 11th Congress of ICAS*, Lisbon, Portugal, Sept. 1978, pp. 333-344.

[3] Johnson, F.T. and Tinoco, E.N., "Recent Advances in the Solution of Three-Dimensional Flows over Wings with Leading Edge Vortex Separations," AIAA Paper 79-0282, 1979.

[4] Lamar, J.E. and Luckring, J.M., "Recent Theoretical Developments and Experimental Studies Pertinent to Vortex Flow Aerodynamics with a View Toward Design," AGARD CP-247, Oct. 1978.

[5] Smith, J.H.B., "Inviscid Fluid Models, Based on Rolled Up Vortex Sheets for Three-Dimensional Separation at High Reynolds Numbers," AGARD LS-94, No. 9, 1977.

[6] Weihs, D. and Boasson, M., "Multiple Equilibrium Vortex Positions in Symmetric Shedding from Slender Bodies," *AIAA Journal,* Vol. 17, 1979, pp. 213-214.

[7] Djojodihardjo, R.H. and Widnall, S.E., "A Numerical Method for the Calculation of Nonlinear, Unsteady Lifting Potential Flow Problems," *AIAA Journal,* Vol. 7, 1969, pp. 2001-2009.

[8] Summa, J.M., "Unsteady Potential Flow About Wings and Rotors Started Impulsively From Rest," *Proceedings of Symposium on Unsteady Aerodynamics,* University of Arizona, Tucson, Ariz., March 1975, pp. 741-767.

[9] Summa, J.M., "A Numerical Method for the Exact Calculation of Airloads Associated with Impulsively Started Wings," AIAA Paper 77-002, 1977.

[10] Atta, E.H., Kandil, O.A., Mook, D.T., and Nayfeh, A.H., "Unsteady Aerodynamic Loads on Arbitrary Wings Including Wing-Tip and Leading-Edge Separations," AIAA Paper 77-156, 1977.

[11] Kandil, O.A., Atta, E.H., and Nayfeh, A.H., "Three Dimensional Steady and Unsteady Asymmetric Flow Past Wings of Arbitrary Planforms," AGARD CP-227, Sept. 1977.

[12] Kandil, O.A., "State of Art of Nonlinear, Discrete-Vortex Methods for Steady and Unsteady High Angle of Attack Aerodynamics," AGARD CP-247, 1978.

[13] Rehbach, C., "Unsteady Calculation of Vortex Sheets Emitted by Highly Inclined Lifting Surfaces," ONERA TP 1978-83, 1978 (in French).

[14] Belotserkovskiy, S.M. and Nisht, M.I., "Modeling of Turbulent Wakes in Ideal Fluids," *Fluid Mechanics—Soviet Research,* Vol. 7, Jan.-Feb. 1978, pp. 102-115.

[15] Katz, J. and Weihs, D., "Large Amplitude Unsteady Motion of a Flexible Slender Propulsor," *Journal of Fluid Mechanics,* Vol. 90, 1979, pp. 713-723.

[16] Katz, J., "Method for Calculating Wing Loading During Maneuvering Flight Along a Three-Dimensional Curved Path," *Journal of Aircraft,* Vol. 16, 1979, pp. 739-741.

[17] Robinson, A. and Laurman, J.A., *Wing Theory,* Cambridge University Press, Cambridge, Mass., 1956.

[18] Drishler, J.A., "Approximate Initial Lift Functions for Several Wings of Finite Span in Incompressible Flow as Obtained from Oscillatory Lift Coefficients," NACA TN-3639, May 1956.

[19] Peckham, D.H., "Low Speed Wind Tunnel Tests on a Series of Uncambered Slender Pointed Wings with Sharp Edges," Aeronautical Research Council, A.R.C. R&M 3186, U.K., 1961.

[20] Tosti, L.P., "Low Speed Static Stability and Damping in Roll Characteristics of Some Swept and Unswept Low Aspect Ratio Wings," NACA TN-1468, 1947.

[21] Wentz, W.H. Jr., "Effects of Leading Edge Camber on Low Speed Characteristics of Slender Delta Wings," NASA CR-2002, Oct. 1972.